5

Polymer Nanocomposite Materials Based on Carbon Nanotubes

Adam J. Proud, Rabin Bissessur and Douglas C. Dahn
University of Prince Edward Island, Canada

1. Introduction

In the past two decades, mobile devices have decreased significantly in size and yet their capabilities and storage capacities continue to grow dramatically. Not unexpectedly, the energy demands of these devices are rather substantial, which has led to a huge increase in the level of research into batteries. In recent years, millions of dollars of research funding have been directed towards the development of more efficient battery systems, with a large focus on lithium ion batteries. These batteries are among the most popular for devices with high energy demands due to their high energy capacities. However, despite the impressive performance of lithium ion batteries to date, there is still significant room for improvement.

Lithium ion batteries have progressed significantly since they were first developed in the early 1970s. These early systems consisted of lithium metal anodes combined with titanium disulfide cathodes; however, they demonstrated limited cell potentials and these chalcogenidic cathodes were soon replaced by layered oxide systems (Whittingham, 1976). Many such layered oxides were studied by the Goodenough group (Thackeray et al., 1983; Mizushima et al., 1980) with great success which led to the commercialization of these batteries in the early 1990s. These batteries were marketed by the electronics giant, the Sony Corporation, and they consisted of a lithium cobalt dioxide, $LiCoO_2$, cathode and a graphitic anode (Nazri & Pistoia, 2004). Lithium metal anodes were discarded earlier in favour of safer systems such as graphite due to the dangers associated with recharging.

In the years since the commercialization of lithium ion batteries, there have been many modifications to the three components of the cell: the anode, the cathode and the electrolyte. However, due to the low cost and relative efficiency of graphite as the anode system, very little work has been done in this area. Nonetheless, recently, silicon and germanium nanowires have demonstrated great potential as possible anode materials (Chan et al., 2008a; Chan et al., 2008b). It has long been known that silicon has a greater capacity for lithium ions than does graphite; however, previous attempts employing silicon particles and thin films have demonstrated significant degradation of the materials upon cycling. With these novel nanowires, this degradation is not observed. A small increase in the diameter of the nanowires occurs upon lithium intercalation, but this expansion is reversible upon the removal of the lithium ions. Research is still continuing into these materials due to their enhanced lithium storage capacities; however, these systems are plagued by their considerable expense when compared to graphite. Therefore,

much of the research into these battery systems has been directed towards the cathode and electrolyte systems.

The cathodes employed in modern lithium ion batteries are far more variable than the anodes. Although layered oxides are among the most common cathode systems, spinels (e.g. manganese spinel) and phospho-olivines (e.g. lithium iron phosphate) have been developed and are currently employed in commercial batteries (Nazri & Pistoia, 2004). These latter two systems are better suited to high current applications where safety is of high concern such as in power drills and electric vehicles.

Electrolytes in lithium ion batteries are traditionally composed of a lithium salt such as $LiClO_4$ or $LiPF_6$ suspended in an organic solvent which is usually a carbonate derivative (e.g. propylene carbonate). These electrolyte systems are by far the most common but there are significant disadvantages to using liquid electrolytes including safety concerns and inflexibility in terms of battery cell shapes. This has led to the development of lithium ion polymer batteries which consist of electrolytes where the lithium salt is suspended in a polymeric matrix. The use of these polymer electrolytes has led to the development of batteries which do not require a metal casing (Nazri & Pistoia, 2004). This in turn, enhances the energy density of the battery, allows for the construction of batteries of varying shape and flexibility, and improves the safety of the cells (Fergus, 2010). This criterion is are well-suited to the ever increasing portability of mobile devices that we are faced with today.

1.1 Solid polymer electrolytes

Traditionally, the polymers used as solid polymer electrolytes in lithium ion batteries were polyethyleneoxide (PEO) and polyacrylonitrile (PAN). However, in the past 20-25 years, numerous compounds have been examined in terms of their properties suitable to polymer electrolytes and it has been found that phosphazenes, such as poly[bis(methoxy-ethoxyethoxy)phosphazene] (MEEP), PEO derivatives, and polysiloxanes have all demonstrated significant ionic conductivities (Allcock et al., 1986; Bouridah et al., 1985; Xu et al., 2001). The properties of a material which typically relate well to potentially high conductivity values include fluidity, amorphousness, and the presence of electron rich centres throughout the material.

Based on molecular mechanics simulations, it is widely believed that lithium ions migrate through an electrolyte by diffusion enhanced by a process known as segmental motion (Meyer, 1998). In this process, lithium ions are thought to coordinate loosely to electron rich atoms or regions along a polymer chain and propagation along the chain occurs by coordinating to electron rich regions further down that chain or a neighbouring chain. Thus, the conductivity of the polymer is significantly affected by the mobility and fluidity of the polymer. Therefore, it is beneficial to explore the use of more fluid (or semi-solid) polymers in order to have a more highly conductive electrolyte. This flexibility correlates well with the glass transition temperatures (T_g) of the polymers. This transition defines the point where a polymer goes from a rigid, glass-like material to a more rubbery, flexible material. Therefore, polymers with low glass transition temperatures are highly desirable due to their more flexible, fluid nature. However, herein lies the problem. The benefits provided by solid polymer electrolytes, including improved safety and adaptable cell shapes, are present due to the solid nature of these materials (Fergus, 2010). Although these problems with mechanical stability are not nearly as severe in comparison to batteries containing liquid electrolytes, they are still significant for those with semi-solid polymer electrolytes. Ionic conductivity in solid polymer electrolytes is not as high as in liquid electrolytes and thus,

without advantages in terms of safety and processability, this form of electrolyte will never be used successfully in commercial batteries.

Improving the mechanical properties of the more highly conductive polymers has been a focal point of research in recent years. The goal is to improve the mechanical stability of the polymer without significantly hindering the conductive properties. Early approaches focussed on chemical cross-linking of the materials. Such methods have been applied to polymers such as MEEP; however, in addition to being far more rigid materials, they are also much less soluble which leads to processing problems (Tonge et al., 1989). In terms of the rigidity, the cross-linking significantly diminishes the mobility of the polymer chains and consequently, the conductivities have suffered greatly.

More recent approaches to improve mechanical stabilities are based on the addition of filler materials to the polymer matrices (Paul & Robeson, 2008). In some cases, especially in crystalline polymers, filler materials can actually increase the conductivity of the material due to the disruption of the crystalline regions resulting in a more amorphous material (Croce et al., 1998). It has been demonstrated that amorphous materials are far more conductive, which is likely due to the increased mobility of the polymer in a less rigid and ordered system. However, in most materials which are originally amorphous, the increased mechanical stability comes at the cost of reduced ionic conductivity (Tonge et al., 1989). The goal is to obtain adequate mechanical stability without sacrificing conductivity to an extent where the polymer is no longer viable as an electrolyte material. These requirements have led to a huge growth in research into nanocomposite materials for use as solid polymer electrolytes.

1.2 Exfoliated nanocomposite materials

With regards to lithium ion batteries, there are two common types of nanocomposite materials that have been explored: intercalated nanocomposites and exfoliated nanocomposites (Figure 1). The latter class of materials are of particular interest due to the significant enhancement of the properties of the polymer materials upon inclusion of only a small quantity of filler material. Additionally, the property enhancement of the resulting material is often greater in these exfoliated compounds compared to their intercalated counterparts.

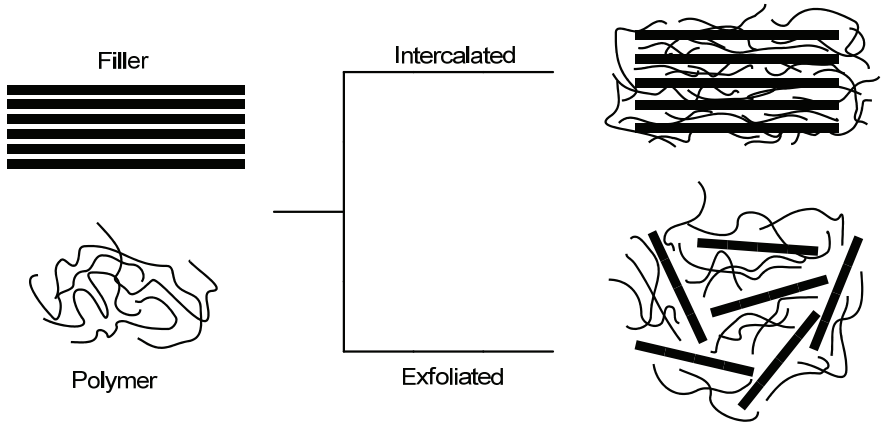

Fig. 1. Schematic representation of the two common forms of nanocomposite materials.

Exfoliated nanocomposites represent a relatively new class of materials (Paul & Robeson, 2008). One of the earliest reports of this class of compound was published by Toyota Central Research and Development Laboratories in 1993 (Kojima et al., 1993). The reported compound was a polymer-clay hybrid material consisting of an exfoliated aluminosilicate structure in the matrix of nylon-6. In comparison to nylon-6, these novel nanocomposites demonstrated improved heat distortion temperatures and elastic moduli.

Since this initial report, countless other exfoliated nanocomposite materials have been synthesized and characterized. These new materials often exhibit improved mechanical, thermal, or conductive properties dependent on the choice of material used as filler and the desired applications. With respect to polymeric materials, these filler materials have ranged from anything from other polymers, to ceramic powders, and more recently to the materials used in this research, carbon nanotubes. While one may not consider the dispersion of nanotubes within a polymer matrix to be a true exfoliated nanocomposite material, it is analogous in many ways which has led to the use of this terminology in this text.

Since their discovery in 1991, carbon nanotubes have been used extensively in countless areas of research (Iijima, 1991; Moniruzzaman & Winey, 2008). These materials (Figure 2) can be either single-walled (SWNTs) consisting of a lone nanotube or multi-walled (MWNTs) which are analogous to a Russian doll set with nanotubes of smaller diameters fitting neatly inside the larger ones (Iijima, 2002). The intertubular spacing is similar to the distance between the sheets of graphite in its 2-D layered structure with a separation of 3.3-3.6 Å. The key features responsible for the remarkable properties of these materials are the high aspect ratios and the highly conjugated network created by the series of fused benzene rings. CNTs have been noted to be stable in air up to temperatures of 700°C and in N_2, the networks are stable beyond 2000°C (Ahir, 2007).

Despite the noteworthy thermal properties, possibly the most attractive properties of CNTs are those pertaining to mechanical strength and stiffness. These properties have led to the belief that nanotubes could potentially be used in fibres for the hypothetical space elevator and are a major reason for the frequent use of these materials in nanocomposites. The Young's modulus, 1.4 TPa, and tensile strength, above 100 GPa, of CNTs are by far the greatest of any known material (Khare & Bose, 2005). For a good comparison, the Young's modulus and tensile strength of high-grade steel are only 200 GPa and 1-2 GPa, respectively. These characteristics could be highly beneficial for improving the mechanical properties of polymer nanocomposites. One such example was reported by Dalton et al. who

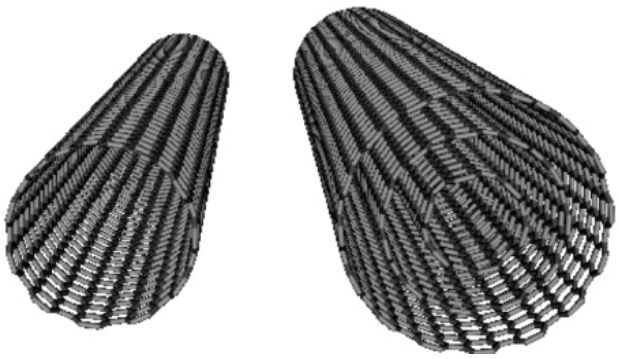

Fig. 2. Molecular model representation of SWNTs (left) and MWNTs (right).

synthesized nanocomposites with 60 wt% SWNTs in poly(vinyl alcohol) which displayed tensile strengths of 1.8 GPa (Dalton et al., 2003). However, ratios of nanotubes used in nanocomposites are often much lower than this in order to retain some desired properties of the polymer. Gao et al. recently synthesized SWNT/nylon-6 nanocomposites with only 5 wt% of the nanotubes (Gao et al., 2005). In this case, increases in Young's Modulus and tensile strength of 153% and 103%, respectively, were observed. The magnitude of the effect of the nanotubes is often related to dispersibility, which leads back to the need for evenly dispersed samples. This has led to varying levels of observed effects on mechanical stability in different studies, but a commonality among all studies has been the improvement of the mechanical properties of the polymer.

As noted, the remarkable thermal, mechanical, and conductive properties of carbon nanotubes make them ideal candidates to be used as filler materials in nanocomposite materials. However, due to the poor solubility of nanotubes, they are difficult to deal with and thus several different methods have been developed and utilized in the preparation of these types of nanocomposites (Ma et al., 2010). Depending on the desired application for the resulting material, the synthetic approach could differ significantly. For example, in a material where one would like to enhance the electrical properties of the material, mechanical processes such as ultrasonication would be better suited than functionalization of the nanotubes. By functionalizing the surface of the nanotubes, the conjugated network of π electrons would be disrupted and the electrical conductivity of the CNTs would decrease significantly. However, for the purposes of this research, this is a desired effect and thus, functionalization was a primary method used for improving the processibility of the nanotubes. By functionalizing the nanotubes, one can hinder the electrical properties of the material while maintaining some of the mechanical and thermal properties.

In addition to functionalization, ultrasonication was also used in the preparation of the materials. As previously mentioned, ultrasonication is ideal for systems where electrical properties are desired, as the conjugated system remains intact, and it has been demonstrated that this mechanical procedure provides sufficient energy to separate the bundles of CNTs to form homogeneous solutions. Care must be taken not to use excessive sonication, as this can significantly decrease the length of the tubes and have a detrimental effect on their properties (Ahir, 2007). Combining the effects from both functionalization and ultrasonication would improve the dispersion of the nanotubes, resulting in a more efficient synthesis since homogeneous dispersion of the filler material is essential to obtain optimal property enhancement in the resulting nanocomposite materials.

2. Synthetic methodology

2.1 Acid oxidation of MWNTs - method 1

The oxidation of carbon nanotubes was performed using commercially available short multi-walled nanotubes (Helix Material Solutions, diameter: 10-30 nm, length: 1-2 μm). The procedure was modified from the method developed by Rinzler et al., for single-walled carbon nanotubes (Rinzler et al., 1998). A sample of MWNTs (1.0 g) was weighed into a 100 mL round bottom flask. Nitric acid (60 mL, 60% by volume) was added to the flask with stirring to disperse the solid. The allotted reaction time was 3 hours. Following the refluxing process, the solid was isolated under reduced pressure and washed with deionized water to remove any traces of HNO_3. Trace moisture was then removed via lyophilisation. This whole process was then repeated once more to improve the solubility of the nanotubes in polar solvents.

2.2 Hummers' oxidation of MWNTs - method 2

The multi-walled nanotubes obtained from Helix Material Solutions were also oxidized via a procedure adapted from Hummers' Method for the synthesis of graphite oxide (Hummers & Offeman, 1958; Liu et al., 2000). A sample of MWNTs (1.0 g) was measured into a 600 mL Erlenmeyer flask to which sulphuric acid (23 mL, 98%) was subsequently added. This solution was stirred while being cooled to 0°C. The oxidizing agent, $KMnO_4$ (3.00 g, 19.0 mmol) was then added over a period of 10 minutes in small increments to prevent the temperature of the reaction from exceeding 20°C. Following the addition of the $KMnO_4$, the reaction flask was removed from the ice bath and allowed to warm to room temperature. Deionized water (23 mL) was then added gradually while ensuring the solution temperature remained below 98°C. The reaction mixture was then left to stir and cool to room temperature over a period of 15 minutes. Finally, deionized water (140 mL) was added in one quick addition followed by the rapid addition of H_2O_2 (10 mL). Upon the addition of H_2O_2, a black precipitate began to form.

The solution was left to stand overnight to allow the precipitate to settle. Once the precipitate had settled, excess solvent was decanted and the remaining solution was swirled to form a slurry. This slurry was then transferred to dialysis tubes to remove any impurities. The dialysis was deemed complete when no precipitate formed upon the addition of $BaCl_2$. Following dialysis, the oxidized nanotubes were isolated by lyophilisation.

2.3 Synthesis of poly[oligo(ethylene glycol)oxalate] (POEGO)

Benzene (99%) and oxalic acid dihydrate were purchased from Sigma-Aldrich while poly(ethylene glycol) (M_n: 380-420) was obtained from EMD Chemical. All chemicals were used without modification. Poly[oligo(ethylene glycol)oxalate] was prepared according to the procedure developed by Xu, et al. (Xu et al., 2001). PEG 400 (2.0 g, 5.0 mmol) was dissolved in benzene (50 mL) in a 250 mL round bottom flask. One molar equivalent of oxalic acid dihydrate (0.63 g, 5.0 mmol) was then added to the solution. The reaction was refluxed with magnetic stirring for a period of 3 days at which point the benzene was removed through rotary evaporation. The remaining product was then heated in a vacuum oven at 120°C for 2 days resulting in a highly viscous, pale-yellow polymer.

2.4 Synthesis of POEGO/LiOTf (LiPOEGO) complexes

POEGO, synthesized as previously described, was complexed with lithium triflate ($LiSO_3CF_3$, LiOTf) in various ratios. The polymer was dried extensively at which point a corresponding amount of LiOTf was added in the inert atmosphere of a nitrogen glove box. The mixture was then transferred to a vacuum oven where it was heated to 90°C overnight. The product was mixed lightly and heated for an additional two hours at 90°C in a vacuum oven.

2.5 Synthesis of MWNT/POEGO nanocomposites - method A

The exfoliated nanocomposites were prepared in both deionized water and acetone. POEGO (0.500 g) was dissolved in the desired solvent (15 mL) and stirred until dissolution was complete. Separately, a sample of oxidized nanotubes (0.0556 g) was dispersed in the desired solvent with the aid of ultrasonication for a period of 2 minutes. After sonication, the two solutions were mixed and the resulting solution was stirred for 24 hours before isolating the final product via lyophilisation (H_2O) or by removing the solvent under reduced pressure (acetone). This produced a polymer nanocomposite material with 10 wt%

MWNTs. This procedure was repeated to produce exfoliated nanocomposites containing 1 wt%, 5 wt%, 15 wt%, and 20 wt% MWNTs. This synthetic procedure was also employed in the preparation of MWNT/LiPOEGO nanocomposite materials.

2.6 Synthesis of MWNT/POEGO nanocomposites - method B

An *in situ*polymerization/nanocomposite preparation was also performed. A sample of oxidized nanotubes (0.111 g) was dispersed in 40 mL of benzene with 20 minutes of ultrasonication. This solution was then added to equimolar amounts of PEG 400 (1.00 g, 2.50 mmol) and oxalic acid dihydrate (0.315 g, 2.50 mmol). The polymerization procedure described in section 2.3 was then applied for the remainder of the synthesis. This yielded a polymer nanocomposite containing 10 wt% nanotubes relative to the quantity of PEG 400 that was used since mass ratios with respect to the polymer could not be determined accurately. This synthetic procedure was repeated to produce exfoliated nanocomposites containing 1 wt%, 5 wt%, 15 wt%, and 20 wt% MWNTs and was also used in the preparation of analogous lithiated samples.

3. Instrumentation

Powder X-ray diffraction (XRD) measurements were performed using a Bruker AXS D8 Advance diffractometer. The instrument was equipped with a graphite monochromator, variable divergence and antiscattering slits, and a scintillation detector. Cu(Kα) radiation (λ=1.542 Å) was used for the measurements. The samples were run in air under ambient conditions from 2-60^{o} (2θ). Sample preparation involved the adhesion of the solid onto double-sided tape adhered to a glass substrate.

Thermogravimetric analyses (TGA) were performed using a TA Instruments TGA Q500 instrument. These analyses were performed under both dry air and dry nitrogen purges. For analyses performed in nitrogen, the furnace was allowed to purge with nitrogen for 20 minutes prior to the commencement of the runs at a rate of 60.00 mL/min. The analyses of these materials were performed at high resolution with a dynamic heating rate. This method of heating utilizes a rate of 10.0°C/min while the weight of the material is roughly constant and the heating rate decreases significantly as the material begins to decompose. The resolution number for these scans was 4.00 while the sensitivity value was 1.00.

Differential Scanning Calorimetry (DSC) analyses of the samples were carried out using a TA Instruments DSC Q100 instrument. Analyses were performed in aluminum pans under a dry nitrogen purge (50.00 mL/min). These analyses were performed using a DSC Heat/Cool/Heat Cycle which observes changes in heat flow versus increasing and decreasing temperatures. Heating rates of 10.00^{o}C/min and cooling rates of 5.00^{o}C/min were used for all samples.

A Bruker Equinox 55 FT-IR instrument with a resolution of 0.5 cm^{-1} was used in the measurement of FTIR spectra for the materials. All samples were run as pressed KBr pellets. A set of 64 background and sample scans were used in determining the spectra. The measurements took place in a chamber which was purged with nitrogen gas at a rate of 8 L/min to eliminate the presence of any CO_2 peaks in the spectra. The chamber was allowed to purge for 20 minutes prior to the commencement of each run.

Nuclear magnetic resonance (NMR) spectroscopy was employed to characterize the polymer samples. A Bruker 300 MHz NMR was used to perform the ^{13}C-NMR and ^{1}H-NMR scans. The measurement of the ^{13}C-NMR spectra involved 1024 scans while the ^{1}H-NMR experiments involved a set of 32 scans. $CDCl_3$ was used as the solvent for all samples.

A Jandel Multi-Height probe was used to perform electrical conductivity measurements. The spacing between the individual probes was 0.1 cm. All samples for measurements were pressed into pellets using a hydraulic press. A Keithley 2000 Multimeter set to 4-probe resistance measurements was then used to measure the resistance of these samples.
Ionic conductivities of the samples were carried out by AC impedance spectroscopy (IS). Due to the thick paste-like nature of these materials, a thin layer was spread evenly on a glass substrate with painted silver electrodes fitted on opposite ends. These samples were dried thoroughly either in a vacuum oven at 120^{o}C for two days (Method 1B) or through lyophilisation for three days (Method 1A and Method 2A) to remove any traces of water which may lead to protonic conductivity. IS was carried out in a vacuum chamber and these samples were held under vacuum for a minimum of 20 hours prior to measurement to remove residual water adsorbed by the samples during their handling after the initial drying process. Throughout the IS measurements, the temperature was controlled using a Lakeshore 321 temperature controller and a Cryodyne 350CP refrigerator. The current flow was directed along the film (i.e. parallel to the substrate). The IS measurements were performed using a Solartron 1250 frequency response analyzer and a home-built accessory circuit for high impedance samples. The frequency range used for most samples was 5 kHz to 0.05 Hz.

4. Results and discussion

4.1 Synthesis and characterization of oxidized nanotubes

Prior to the preparation of the exfoliated nanocomposite materials, the synthesis and complete characterization of the filler material was required. Due to the electrically conductive nature and poor solubility of carbon nanotubes, the materials required processing before they could be incorporated into the polymer matrix for potential use as solid electrolyte materials. One such approach is that of oxidation which was carried out here. Two separate approaches were used in the oxidation of the CNTs. The first approach (Method 1) involved refluxing the nanotubes in concentrated acid solutions as previously described (Section 2.1), while the other approach (Method 2) involved an adaptation of Hummers' Method (Section 2.2) which was designed for the synthesis of graphite oxide.

Wavenumber (cm^{-1})	Designation
3431.6	O-H stretch
1721.4	C=O of ketone
1634.0	C=O stretch of carboxylic acid
1094.7	C-O stretch

Table 1. IR absorptions in Hummers' Oxidized MWNTs

The oxidized nanotubes prepared via Method 1 were characterized by FTIR spectroscopy; however, the spectrum did not provide sufficient evidence for oxidation. This may be expected due to the nature of the oxidation process. It is known that oxidation by refluxing in acidic solutions leads to the opening and shortening of the nanotubes with the oxidative functionalities occurring primarily at the tips of the nanotubes. Thus with minimal oxygen containing functional groups in a longer nanotube, IR spectroscopy was deemed an inefficient method of characterization. However, with regards to the nanotubes oxidized by

the Hummers' Method adaptation, IR did prove to be more effective. The IR spectrum indicated several oxygen containing functionalities which are tabulated in Table 1.
Due to the inefficacy of IR measurements for the acid oxidized nanotubes, other methods of characterization were carried out. One such method was thermogravimetric analyses (TGAs) which were performed on the untreated nanotubes, the nanotubes that were oxidized twice by acid, and the Hummers' oxidized nanotubes. These TGAs were carried out in nitrogen as all nanotubes, regardless of the level of oxidation, would completely degrade in an oxygen atmosphere. As can be seen from the traces in the thermogram in Figure 3, the untreated nanotubes displayed very minimal decomposition with a total weight loss of less than 2% which can be attributed to impurities in the nanotubes from the method from which they were synthesized. The acid oxidized nanotubes demonstrated a greater weight loss with overall decomposition accounting for approximately 7% of the material, whereas the Hummers' oxidized nanotubes degraded further still with less than 60% of the material remaining after heating up to 800°C. This greater extent of oxidation is expected from the results previously described from the IR analyses. This greater level of oxidation is advantageous in terms of increased solubility and decreased electrical conductivity; however, the mechanical integrity of these nanotubes would likely be decreased.

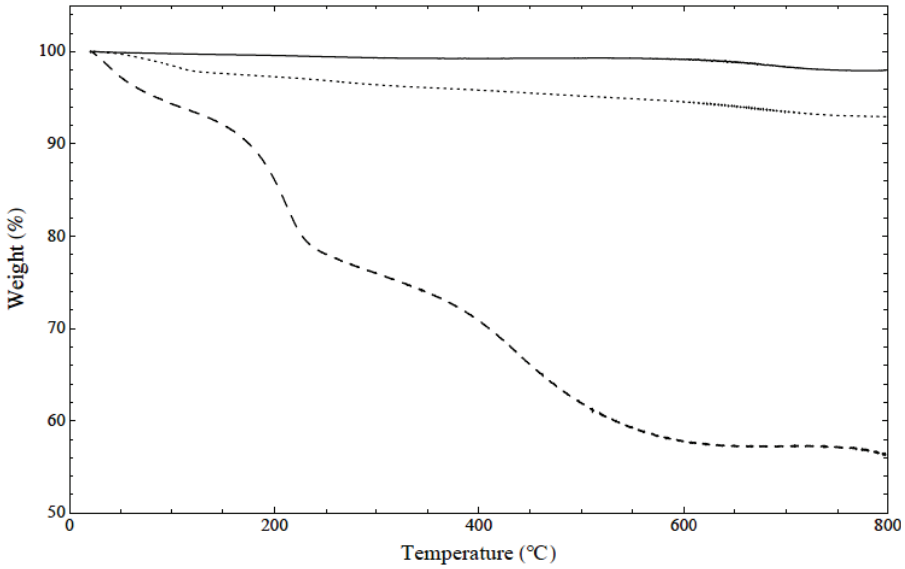

Fig. 3. TGA comparison of untreated MWNTs (solid), acid oxidized MWNTs (dotted), and Hummers' oxidized MWNTs (dashed).

Further structural information regarding these nanotubes was provided by XRD analyses. Again, the untreated, acid oxidized, and Hummers' oxidized nanotubes were characterized for comparative analysis (Figure 4). The untreated nanotubes display one main peak in the diffractogram with a d-spacing value of 3.4 Å. This value likely corresponds to the spacing between the individual nanotubes within a single MWNT. This peak is present in the acid oxidized nanotubes denoting that this oxidative method does not significantly alter the

structure of the MWNTs. Considering acid oxidation results in oxidation primarily at the tips of the nanotubes, this is not unexpected. However, with the nanotubes oxidized using the harsher Hummers' method, this peak is still present, but not nearly as prominent as it was in the other two samples. Instead, the diffractogram is indicative of a primarily amorphous material. This likely indicates that the order of the MWNTs was disturbed in the oxidation process. Normally, the nanotubes are consistently separated by this intertubular distance of 3.4 Å; however, it is possible that these harsher oxidizing conditions could have introduced functionalities on the outer walls of the nanotubes which would disturb this regular spacing.

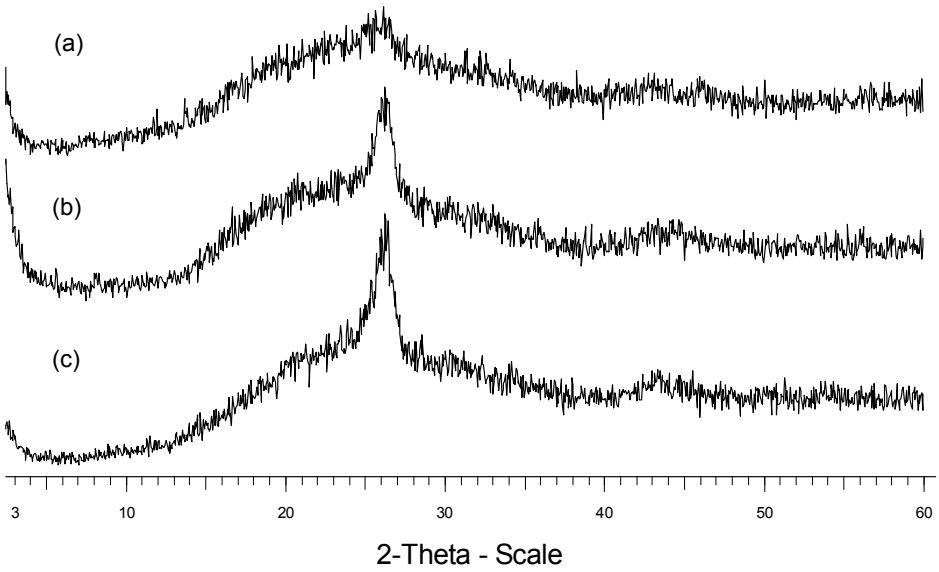

Fig. 4. Diffractogram of (a) Hummers' oxidized MWNTs, (b) Acid oxidized MWNTs, (c) Pure MWNTs.

The final, and potentially most important, method of characterization for these oxidized nanotubes was that of four-probe electrical conductivity measurements. As previously mentioned, due to the electrically conductive nature of the nanotubes, oxidation was required to disrupt the conjugated network of π electrons and inhibit conductivity in order for these nanocomposite materials to potentially be used as solid polymer electrolytes. In obtaining these measurements, pressed pellets of each of the materials were prepared using a hydraulic press and pressures of 6000 psi. Co-linear four-probe electrical conductivity measurements of each sample were then conducted, at room temperature, and the conductivity was determined by

$$\sigma = \ln(2)/\pi\, R\, w \tag{1}$$

where σ and R are the electrical conductivity and resistance of the sample, respectively, and w is the thickness of the pellet (Hall, 1967). Using this expression the conductivities of the untreated, acid oxidized, and Hummers' oxidized nanotubes were determined. These values are summarized in Table 2. It should be noted that as the measurements were made on

pressed pellets, the presence of grain boundaries would lead to some error in the results. Nonetheless, it provides a good method for comparison to demonstrate the decreased conductivity in the oxidized samples.

Sample	Thickness (cm)	Resistance (Ω)	Conductivity (Scm^{-1})
MWNT pure	0.0500	4.40	1.0
Oxidized MWNT (Method 1)	0.0500	15.3	0.29
Oxidized MWNT (Method 2)	0.0087	1779	0.014

Table 2. Electrical Conductivity of MWNT samples

The nanotubes that were oxidized in acid (Method 1) displayed roughly a 3-fold decrease in conductivity, while those that were oxidized by Hummers' Method (Method 2), which demonstrated significant structural differences as evidenced by previous characterization, displayed a far greater 70-fold decrease. Despite the much greater decrease in conductivity for the oxidized nanotubes prepared by Method 2, many of the results for the nanocomposites are based on those prepared by Method 1, due to the current uncertainty regarding the mechanical and structural properties of those nanotubes that underwent the harsher oxidation method.

4.2 Characterization of poly[oligo(ethylene glycol)oxalate] (POEGO)

To date, the research conducted into the use of POEGO as a potential solid polymer electrolyte has been very limited, despite the fact that room temperature ionic conductivities of the polymer rival those of PEO. For this reason, we have decided to explore the conductive properties of this material upon complexation with lithium triflate (LiOTf), in addition to the effects on these properties, and others, due to the addition of the filler nanotubes.

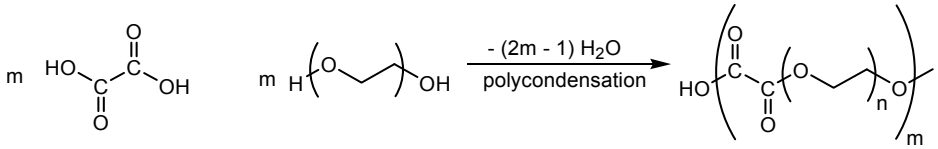

Fig. 5. Reaction scheme for the synthesis of poly[oligo(ethylene glycol)oxalate].

POEGO was synthesized according to the procedure outlined in the experimental section, after which it was characterized both structurally and thermally through a variety of techniques. These include FTIR, NMR, DSC, TGA, and XRD. Based on the reactants used in the preparation of the polymer, in addition to the expected structure (Figure 5), FTIR spectroscopy provides good evidence for the successful formation of the material through the presence of absorption peaks characteristic of hydroxyl groups, carboxyl groups, and esters among others. The characteristic peaks of the polymer are summarized in Table 3. It is known that unreacted PEG often remains following the synthesis of POEGO; however some key features which distinguish it from the starting polymer, PEG, include the carboxyl groups of the carboxylic acid as well as the esteric C=O groups.

^{1}H-NMR and ^{13}C-NMR were also employed in the characterization of the polymer providing further evidence of a successful synthesis. The results of these analyses are tabulated in Table 4. Some peaks that were present in the spectra were indicative of unreacted PEG 400 which is consistent with previous results in the literature (Xu et al. 2001).

Wavenumber (cm^{-1})	Designation
3489.9	OH stretch
2882.6	sp^3 C-H stretch
1765.2	C=O stretch of carboxylic acid
1760.3	C=O stretch of ester
1196.7/1099.6	C-O stretch of ester/ether/alcohol

Table 3. IR absorptions in POEGO

^{1}H-NMR	δ (ppm)	Designation
	4.42	-C(O)-C(O)-O-CH_2-
	3.78	-C(O)-C(O)-O-CH$_2$-CH_2-
	3.73	unreacted PEG 400
	3.65	-C(O)-C(O)-O-CH$_2$-CH$_2$-(OCH_2CH_2)$_{n-2}$-O-
^{13}C-NMR	**δ (ppm)**	**Designation**
	157.97	-*C*(O)-*C*(O) -
	72.90	unreacted PEG 400
	70.90	unreacted PEG 400
	70.62	-C(O)-C(O)-O-CH$_2$-CH$_2$-(OCH$_2$CH$_2$)$_{n-2}$-O-
	68.75	-C(O)-C(O)-O-*C*H$_2$-
	66.31	-C(O)-C(O)-O-CH$_2$-*C*H$_2$-
	62.01	unreacted PEG 400

Table 4. ^{1}H-NMR and ^{13}C-NMR Data for POEGO

The last form of structural analysis used in characterizing the polymer was a powder X-ray diffraction measurement. This was used to determine the crystallinity of the material. From this analysis, POEGO appeared to be an amorphous material which is consistent with its high ionic conductivity. This analysis was essential to verify the amorphous nature of the material considering its precursor, PEG/PEO, is known to be a semicrystalline material in some temperature ranges. As previously noted, amorphous materials are far more conductive than their crystalline counterparts due to the increased mobility of the polymeric chains in a less ordered system (Meyer, 1998).

With the IR, NMR, and XRD data confirming the successful synthesis of POEGO, the thermal analyses of the material provided data concerning the thermal properties of this polymer. Specifically, in terms of the flexibility or fluidity, and in turn, the conductivity of these materials, we are interested in the glass transition temperatures, T_g, of the polymeric materials, and how they are affected upon complexation with lithium salts or the addition of the nanotube filler material. Through DSC analysis, the glass transition temperature for POEGO was determined to be -56.7°C (Figure 6), which compares well to the literature value of -55°C. The minimal difference in these values can be accounted for by slight differences in the degree of polymerization as well as the method utilized to determine the onset of the glass transition temperature. It should be noted that the glass transition temperature was taken at the onset of the transition to be consistent with the literature. Later in the chapter, oftentimes only the midpoint of the T_g will be provided. This low glass transition temperature is ideal for an ionically conductive polymer since the polymeric chains would remain mobile and flexible even at low temperatures. Once the polymer is complexed with LiOTf or the nanocomposite materials with nanotubes are prepared, this glass transition temperature is expected to increase slightly; however, these results will be explored in depth later in this chapter.

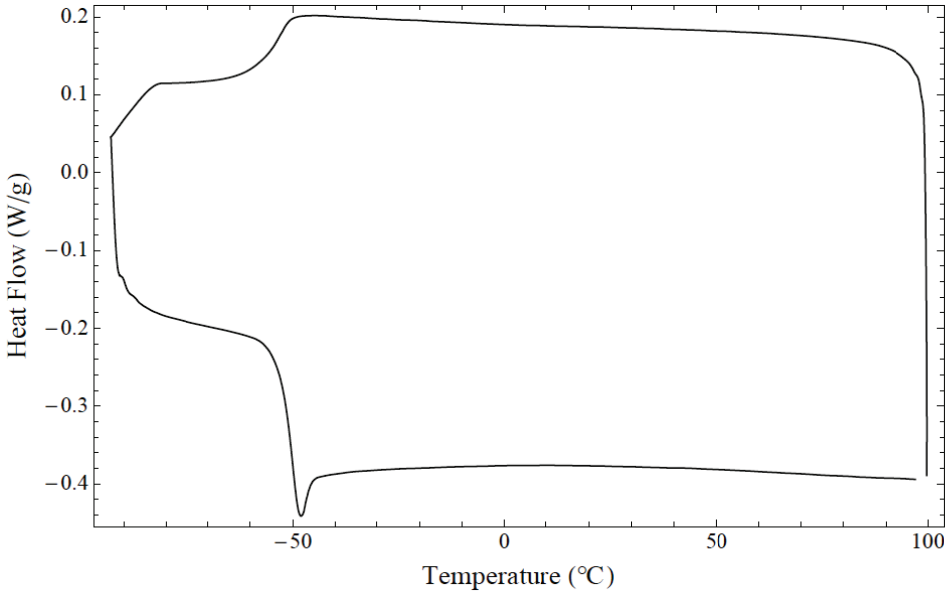

Fig. 6. DSC trace of poly[oligo(ethylene glycol)oxalate].

The final form of analysis used to characterize this polymer was thermogravimetric analysis to determine the thermal stability of the polymer for later comparison. These analyses were performed in both dry air and dry nitrogen atmospheres and it was found that the polymer was stable beyond 170°C in both environments. This level of thermal stability is more than adequate for a component of a battery system; however, despite the fact that this system was geared towards use as a solid polymer electrolyte, it could potentially find uses in other areas as well. Thus it is essential to determine the thermal stability of the material and what potential beneficial effects the filler nanotubes could provide to the resulting nanocomposite. The TGA traces conducted in air and N_2 indicated that the polymer is stable up to 221°C in a nitrogen atmosphere. This represents a 45°C increase over the initial temperature of decomposition, T_d, of POEGO in air. Beyond 400-500°C, the polymer had effectively decomposed entirely under both sets of conditions. These thermal stabilities are more than adequate for a material intended to be used as a solid polymer electrolyte.

4.3 Characterization of LiOTf/POEGO (LiPOEGO)

As previously mentioned, the data available in the literature on the thermal and conductive properties of POEGO is fairly limited. Much of the data concerning the ionic conductivity of the polymer is for higher molecular weights of POEGO which was complexed with lithium salts with larger anions such as lithium bis-(trifluoromethanesulfonyl)imide (LiTFSI); therefore, we chose to synthesize a range of lithiated polymers with different ratios of polymer to salt. From the published data and from knowledge of POEGO salt complexes from previous work done in our group, the ratios of [Li]/[EO] that were studied were 1:8, 1:12, 1:16, and 1:20 (Xu et al., 2001). [1]

[1] [EO] - the etheric unit of POEGO

These polymer salt complexes underwent characterization to determine the effects of the salt on the thermal and structural properties of the polymer. Of particular interest was the effect of the salt on the glass transition temperature of POEGO. One would expect that the T_g would increase upon the addition of salt which would have a detrimental effect on conductivity; however, adequate quantities of the salt would be required in order for conductivity to be sufficient. Thus these two competing effects were analyzed in the characterization of the polymer to determine the optimal ratio.

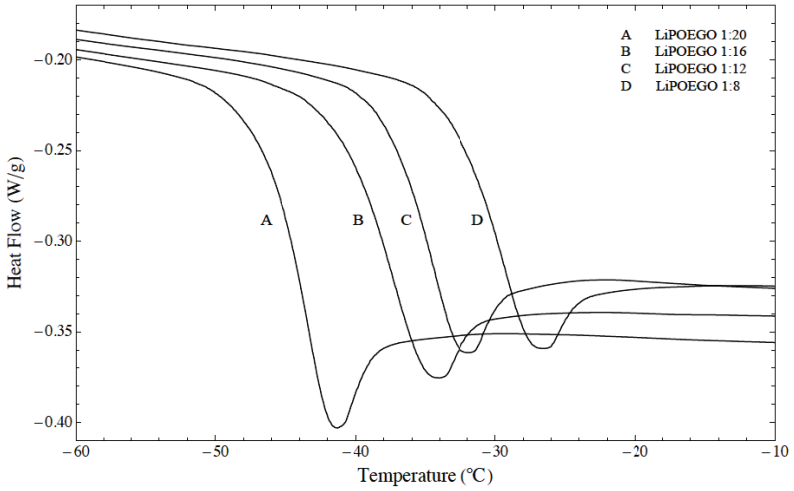

Fig. 7. DSC traces outlining the T_g of LiOTf/POEGO complexes of varying ratios.

In Figure 7, the DSC of the polymer/salt complexes for the four ratios of interest are displayed. As expected, we see an increase in the glass transition temperature upon the introduction of greater quantities of the salt. The midpoint of the T_g increases from -44.0°C for the 1:20 ratio up to -30.7°C for the sample with the highest salt concentration, 1:8. The results for the series of polymer complexes are listed in Table 5.

[Li]/[EO]	Onset of T_g (°C)	Midpoint of T_g (°C)
1:8	- 36.5	- 30.7
1:12	- 40.7	- 35.6
1:16	- 44.6	- 38.2
1:20	- 50.8	- 44.4
0	- 56.7	- 50.7

Table 5. Effect of Salt Concentration on T_g of POEGO

To ensure that complexation had been successful and the salt had efficiently dissociated within the polymer matrix, XRD analyses were carried out. Based on the nature of LiOTf, it is expected to be a highly crystalline material. This was confirmed by a series of sharp peaks present in the diffractogram (Figure 8). This was highly beneficial in determining the efficacy of the polymer salt complexes. With proper dissociation of the salt, combined with the amorphous nature of the polymeric material, it is expected that the diffractogram for the polymer/salt complexes should also be amorphous. The XRD for these materials confirmed this hypothesis with the samples of all ratios presenting a completely amorphous pattern.

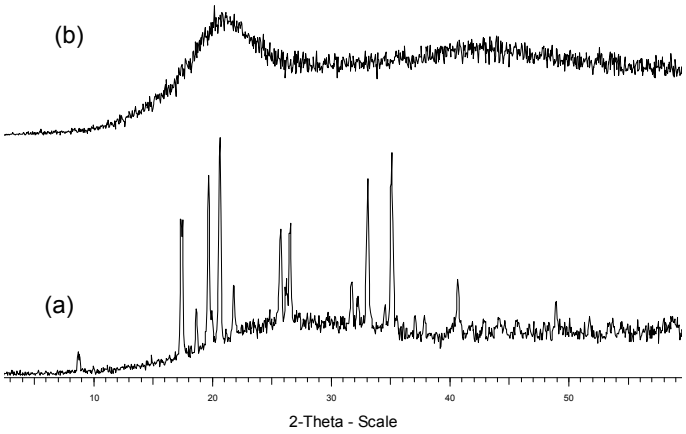

Fig. 8. XRD comparison of (a) crystalline LiOTf, and (b) amorphous LiPOEGO 1:8.

Thermal analyses of both the LiOTf and LiOTf/POEGO complexes were carried out by means of TGA to see what effect, if any, the salt had on the thermal stability of the polymer. It was found that lithium triflate begins to degrade at temperatures greater than 400°C; however, the effect of the salt on the onset temperature for the degradation of the polymer is negligible. In the polymer/salt complexes, we observe two main decomposition steps; the first occurring around 225°C denotes the degradation of the polymer while the second step begins around 418°C which corresponds largely to the decomposition of the triflate ion.
The final and most important method of characterization for the polymer/salt complexes was that of ionic conductivity measurements. Through these analyses, it was discovered that the optimal [Li]/[EO] ratio is 1:16 as expected from the literature results (Xu et al., 2001). With this ratio, the polymer had measured ionic conductivity values on the order of 10^{-6}-10^{-5} S/cm with temperatures ranging from 290-320 K which compares well to the previously reported values. These results are summarized below in Table 6. Using this information, the exfoliated nanocomposites synthesized for conductivity testing were prepared using the same 1:16 ratio.

[Li]/[EO]	Temperature (K)	Ionic Conductivity (S/cm)
1:16	290	2.9×10^{-6}
1:16	300	8.1×10^{-6}
1:16	310	1.9×10^{-5}
1:16	320	4.1×10^{-5}

Table 6. Ionic conductivity data for LiOTf/POEGO complex.

4.4 Characterization of the exfoliated nanocomposites

The most integral part of this research was developing the synthetic methodology and fully characterizing the polymer nanocomposites containing MWNTs as filler materials. Two main approaches were employed in the synthesis of these novel materials. The first method (Method A) is that which is commonly seen in the literature and involves the dispersion of the nanotubes in water via ultrasonication which is then mixed with a solution containing the desired polymer.

Mass Percent	ΔT_g (°C)			
	Method 1A[2]	Method 1A[3]	Method 2A[2]	Method 1B
1	- 0.71	+ 0.29	- 5.12	+ 1.12
5	- 1.46	+ 0.57	- 4.12	+ 0.55
10	- 0.57	- 0.42	- 1.70	+ 1.68
15	+ 1.62	+ 1.00	- 2.56	+ 0.69
20	+ 0.01	+ 0.77	- 0.57	+ 2.11

Table 7. ΔT_g (°C) of MWNT/POEGO complexes.

Samples prepared by this method used both acid oxidized nanotubes (Method 1A) and Hummers' oxidized nanotubes (Method 2A). Each of these samples was characterized by both DSC and TGA to determine the effect of the filler material on the thermal properties of the polymer. As previously demonstrated, when POEGO was mixed with LiOTf at any ratio, we saw an increase in the T_g of the polymer. Thus, it was expected that a similar increase would be observed upon the addition of the MWNTs to the polymer matrix. However, interestingly enough, this was not observed in some cases and instead decreases in T_g were recorded. Even at the higher loadings of MWNTs (i.e. 15-20 wt%), a slight decrease in T_g was observed in some cases as noted in Table 7.

As the glass transition temperature of POEGO can vary slightly with each synthesis, it was determined that ΔT_g would be a better method of comparison for the nanocomposites prepared by each of the different methods. With regards to the samples prepared by the *in situ* synthesis (Method 2A), the reference for comparison is the midpoint of the glass transition temperature previously recorded in this chapter (-50.7°C).

These decreases in the glass transition temperature led to further examination of the method of preparing the nanocomposites. First, the samples were prepared in a more volatile solvent (acetone) to determine whether or not trace water in the final products was causing this decrease in T_g. In addition to alternative solvents, an *in situ* preparation (Method 1B) was utilized not only to eliminate the use of water as a solvent, but also to potentially improve the dispersion of the nanotubes in the polymer matrix by adding them before the polymerization occurs. It should be noted that the *in situ* preparations were only performed with the nanotubes oxidized by acid (Method 1) due to the complete insolubility of the Hummers' oxidized nanotubes in benzene. The data appear to suggest that the samples prepared in water may be absorbing water which leads to the decrease in the glass transition temperature. However, it could also be a result of the disruption of the crystallinity of the unreacted PEG remaining in the polymer matrix. This disruption of the crystalline regions could lead to a decrease in the glass transition temperature counteracting the expected increase in the glass transition temperature due to the decreased mobility of the polymer chains in the more solid-like nanocomposite material (Zeleznak & Hoseney, 1987). This effect would be more dramatic in the materials prepared in water due to the much greater solubility of the oxidized nanotubes in water compared to acetone and benzene. This improved solubility would likely lead to better dispersion of the nanotubes in the polymer matrix and thus a more efficient disruption of the crystalline PEG.

A first glance at the table of data may raise some concerns as there does not appear to be any pattern in terms of the effect on the T_g of the nanocomposites. However, with several competing effects in terms of residual solvent content, disruption of crystallinity, and

[2] Samples prepared in H_2O

[3] Samples prepared in acetone

increased solid character, slight variations in any of these effects between samples would cause slight differences in the transition temperature. One might suggest that the only reason for the decreases in T_g is due to residual water; however, TGA analyses (see below) have demonstrated that all samples, regardless of the method of preparation, contain roughly equivalent amounts of solvent (~0.5-1.5 wt%). The key feature to note here is that none of the nanocomposite materials display major increases in the glass transition temperature which suggests that the ionic conductivity of the materials may not be significantly diminished due to the presence of the mechanically stabilizing nanotubes.

Another feature of these polymer nanocomposites that was examined was their thermal stability. In fact, this was the method used to determine the optimal conditions for the preparation of these materials. As previously mentioned, sonication can have a detrimental effect on the length and mechanical properties of the MWNTs. However, without adequate levels of sonication, the nanotubes do not disperse well in the solvents employed in this study, and thus thermal analyses of the resulting nanocomposites were performed to determine the optimal sonication time to provide adequate dispersion without significantly degrading the nanotubes. Sonication times of 0.5, 1, 2, 5, and 10 minutes were tested for nanocomposite materials containing 10 wt% MWNTs which were prepared by Method 1A. The results of these experiments are displayed in Figure 9. As demonstrated by the plot, the optimal sonication time was determined to be 2 minutes and thus, this length of sonication was utilized for preparation of all samples. The dashed line denotes the thermal stability of POEGO by itself (T_d = 220.92°C).

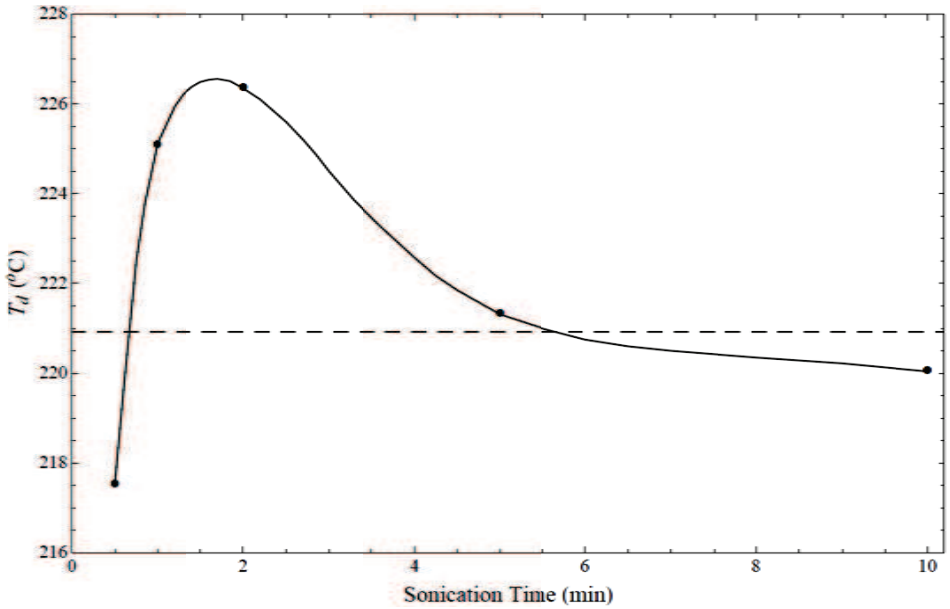

Fig. 9. Effects of sonication time on the thermal stability of polymer nanocomposites.

Using this optimized procedure, the samples of all methods were prepared and analyzed in terms of their thermal stabilities. These results are summarized in Table 8. As was the case with the DSC analyses, the parameter of interest here is ΔT_d due to slight variations in the decomposition temperature with each synthesis of POEGO. The reference for comparison

for the nanocomposites prepared from Method 1B is that which was previously discussed in this text (T_d = 220.92°C).

Mass Percent	ΔT_d (°C)			
	Method 1A[4]	Method 1A[5]	Method 2A[4]	Method 1B
1	+ 1.04	+ 0.54	- 3.76	+ 4.19
5	- 1.51	- 0.53	+ 2.30	+ 2.38
10	+ 5.43	- 1.11	+ 0.39	+ 6.84
15	+ 0.65	- 1.86	+ 3.43	+ 4.95
20	+ 0.16	+ 0.03	+ 3.06	+ 7.22

Table 8. ΔT_d (°C) of MWNT/POEGO complexes.

Once again, there does not appear to be observable patterns in the thermal stabilities of these materials. One of the greatest increases in thermal stability (ΔT_d = 5.43°C) is that of the sample for which the process was optimized (Method 1A - 10 wt%). This sample was set as the benchmark for all of the others based on the fact that it was the sample with the lowest loading capacity which began to gain the dimensional stability of a solid. The samples containing 5 wt% of MWNTs appeared to be more solid than POEGO; however, they still had a slight tendency to flow like a glutinous material.

It is possible that if the process was optimized for every sample, the thermal stabilities of the materials would improve upon those which were observed here. The samples prepared by Method 1B appear to be the best in terms of thermal stability; however, these results must be interpreted with caution. There are two possible explanations for these results. The first is that of the improved dispersion of the nanotubes within the polymer matrix due to the presence of the nanotubes during the polymerization process. The other explanation is that with separate syntheses, the thermal stability of POEGO will vary to some extent and thus a portion of this improvement in thermal stability could be due to an increase in the stability of the POEGO itself.

While these thermal analyses are an important method of characterization for these materials, for a polymer nanocomposite which is thermally stable beyond 200°C, this is more than sufficient for a material with a desired application as a solid polymer electrolyte. If the desire was to significantly improve the thermal stability of a specific polymer, oxidation of the nanotubes would not be the ideal synthetic method unless subsequent reduction with hydrazine was conducted.

The final methods of characterization for these nanocomposite materials involved FTIR and XRD analyses to ensure that the nanotubes were not degraded during the synthesis of these materials and to observe whether interactions between the polymer and the filler occurred.

The IR analyses were conducted to observe what effect, if any, the filler nanotubes have on the vibrations of the functional groups within the polymer. There have been reports in the literature which have assessed the effects of a filler material by observing shifts in the vibrations in the IR spectrum (Zhang et al., 2007). Analogous analyses were conducted here as the vibrations of POEGO were compared to those in the exfoliated polymer nanocomposites. Untreated nanotubes would likely interact very weakly with the polymer; however, the oxidation process creates the possibility for hydrogen bonding between the MWNTs and the polymer matrix. Another property of these materials to consider is their

[4] Samples prepared in H_2O

[5] Samples prepared in acetone

increased rigidity due to the presence of this material. This rigidity could also shift the frequency of the vibrations which can be observed in their respective IR spectra. The summary of these results for a nanocomposite containing 10 wt% nanotubes prepared by Method 1A is listed in Table 9. Many of these shifts are between 5 and 20 wavenumbers as expected as the interactions between the filler and polymer would not be strong enough to cause major shifts. The vibration for the O-H stretch appears to be shifted significantly; however, this could be due to differences in residual water either in the materials themselves or in the KBr used to prepare the pellets for measurement.

POEGO v (cm^{-1})	MWNT/POEGO v (cm^{-1})	Δv (cm^{-1})	Designation
3489.9	3397.6	- 92.3	O-H stretch
2882.6	2877.7	- 4.9	sp^3 C-H stretch
1760.3	1745.7	- 14.6	C=O stretch of carboxylic acid
1196.7	1177.3	-19.4	C=O stretch of ester
1099.6	1104.4	+ 4.8	C-O stretch of ester/ether/alcohol

Table 9. FTIR wavenumber shifts in polymer nanocomposites.

As previously discussed, POEGO is an amorphous material while the oxidized nanotubes display a peak in the diffractogram corresponding to the intertubular spacing of 3.4 Å. The diffractograms for the nanocomposite materials also contain a peak with low intensity corresponding to this same spacing (Figure 10). TGAs of the nanocomposite materials were conducted in order to decompose the polymer and observe whether the nanotubes remain throughout the synthetic process. XRDs were conducted on the remaining material which showed significant increases in the intensity of the lone peak indicating that the structure of the nanotubes are still intact upon incorporation into the polymer nanocomposites. This change in intensity can be attributed to the decomposition of the amorphous polymer network and thus the relative strength of this reflection increases.

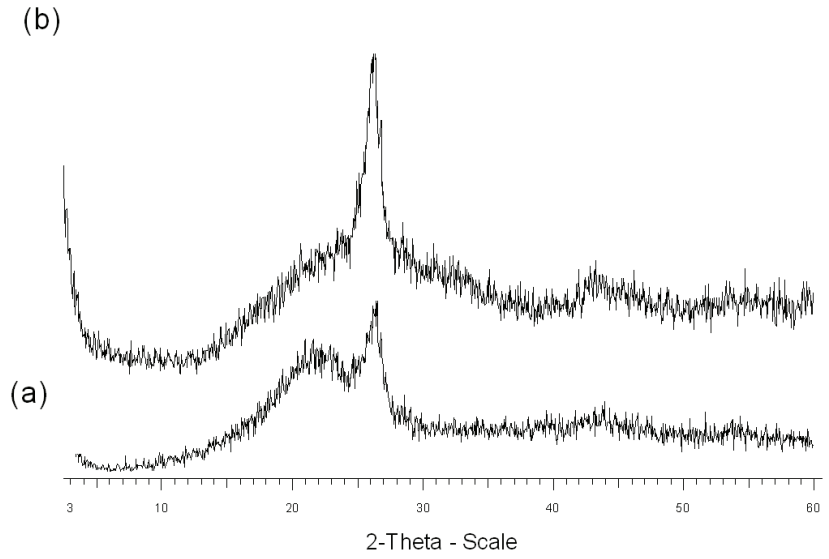

Fig. 10. Diffractogram of (a) 20 wt% nanocomposite before heating, (b) after heating to 800 °C.

4.5 Ionic conductivity results for polymer nanocomposites

The final method of characterization for these nanocomposite materials was that of AC impedance spectroscopy to determine their ionic conductivity properties. The samples were prepared and run as outlined in section 3. The thickness of each sample was estimated at 0.0055 cm (±0.001 cm). The sample width and length varied slightly with each sample and are summarized later in Table 10.

From these analyses, it was determined that the conductive properties of the materials were largely dependent on the method of preparation. The samples prepared by Method 1A appeared to be either electrical conductors or mixed electrical/ionic conductors. This was apparent from the Nyquist plot as the impedance Z went to the real axis and stayed there at lower frequencies, which is characteristic of an electrical conductor. (The resistance of the sample in parallel with cable capacitance produces a semi-circular impedance arc characteristic of a simple RC network). For an ionic conductor between blocking electrodes, the imaginary part of the impedance goes through a minimum known as the touchdown point and then begins increasing again as the frequency continues to decrease. The ionic resistance of the sample was taken to be the real part of the impedance at the touchdown point. Examples of both types of Nyquist plot are displayed in Figure 11.

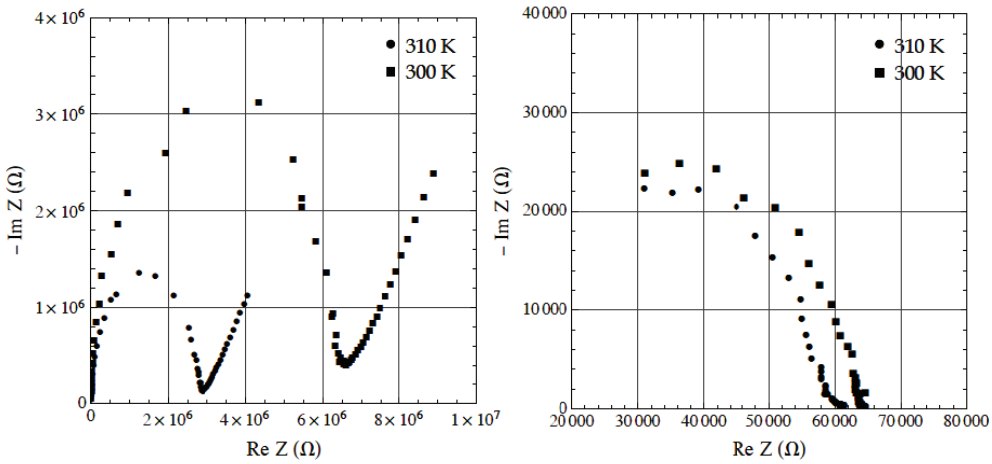

Fig. 11. Examples of Nyquist plots of ionic (left) and electrical/mixed conductors (right). High frequencies yield the points on the left of each plot; low frequencies are on the right.

After concluding that the samples prepared by Method 1A did have properties of electronic conductors through analyses of the 10 wt% and 20 wt% samples, no additional samples were measured by AC impedance spectroscopy. Although these materials could potentially be used in other fields, this electrical conductivity would prohibit their use as electrolyte materials, which are required to be electrical insulators. The samples prepared by Method 2A were more interesting. These samples, as previously mentioned, involved the mixing of the oxidized MWNTs during the polymerization process. At a low loading capacity of 5 wt%, this sample appeared to be an efficient ion conductor. This was evidenced in the previously shown Nyquist plot as well as the following plots of conductivity versus temperature. In this type of plot, the conductivity of the ionic conductors tends to increase almost exponentially with temperature, resulting in a linear trend when the data is

displayed as a semi-log plot. Electrical conductors do not see as dramatic of an increase in conductivity with increasing temperatures. The conductivity results are summarized in Figure 12 as well as in Table 10. The box in the table outlines the conductivities of the samples which are solely ionic conductors.

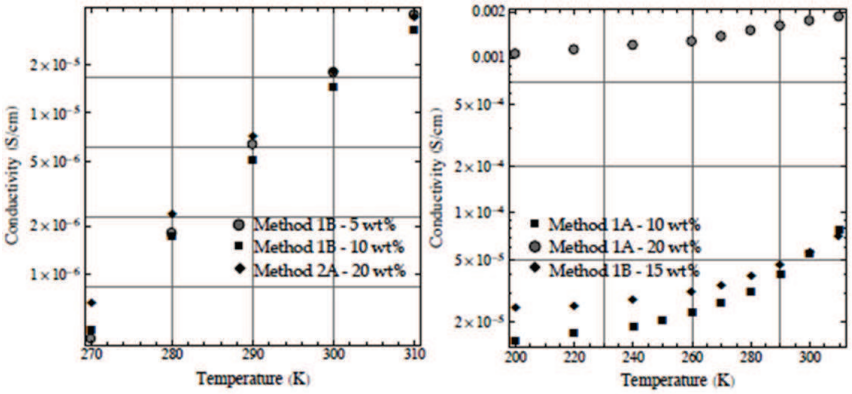

Fig. 12. Semi-log plots of conductivites of ionic conducting (left) and mixed conducting (right) polymer nanocomposite samples at various temperatures.

From the data presented in Figure 12, more evidence is provided that the samples prepared by Method 1A are electrical conductors as previously observed with the Nyquist plots. However, the plots of conductivity versus temperature are relatively flat at low temperatures, but as the temperature increases past 260 or 270K, the slopes of the lines increase observably. This suggests that these materials are mixed conductors. At higher temperatures, when the polymer is more fluid, ionic conductivity becomes a more important factor; however, at the lower temperature range when the mobility of the polymer chains decreases significantly, electrical conductivity becomes the major contributor to the conductivity of the samples.

Sample	Sample Dimensions (cm)		Conductivity (S/cm) (± 20%)		
	Width	Length	290 K	300 K	310 K
Method 1A - 10 wt%[6]	0.889	0.635	4.0×10^{-5}	5.4×10^{-5}	7.9×10^{-5}
Method 1A - 20 wt%[6]	1.003	0.610	1.6×10^{-3}	1.8×10^{-3}	1.9×10^{-3}
Method 2A - 20 wt%	0.876	0.584	**7.1×10^{-6}**	**1.8×10^{-5}**	**3.9×10^{-5}**
Method 1B - 5 wt%	0.980	0.610	**6.4×10^{-6}**	**1.8×10^{-5}**	**4.1×10^{-5}**
Method 1B - 10 wt%	0.927	0.610	**5.1×10^{-6}**	**1.5×10^{-5}**	**3.2×10^{-5}**
Method 1B - 15 wt%[6]	0.876	0.584	4.6×10^{-5}	5.6×10^{-5}	7.0×10^{-5}

Table 10. Conductivities of polymer nanocomposite materials.

When AC impedance spectroscopy was performed on the LiPOEGO samples (Table 6), the accuracy was estimated at ±50% due to the non-uniform thickness of the films and the estimation of the density of the materials. Here, the uncertainty was estimated at ±20% mainly

[6] Mixed electrical/ionic conductors.

due to the uncertainty in the thickness of the films as previously discussed. Three of the samples listed above (boxed, bolded area) are solely ionic conductors which makes them possible candidates to be used as solid polymer electrolytes. In comparison to LiPOEGO itself, the conductivities of these samples are very comparable. In fact, these values are actually higher than those previously recorded for LiPOEGO. However, when the uncertainties combined with the slightly greater possibility of proton conduction in these samples are taken into account, it is probable that the conductivity values of LiPOEGO and those of the polymer nanocomposites are very similar. This supports the hypothesis that the decreases in glass transition temperatures in the polymer nanocomposites were likely due to a disruption of any crystalline regions of the material. This would lead to an improvement in conductivity counteracting the expected decrease in conductivity due to the increased rigidity of the materials.

5. Conclusion

Exfoliated nanocomposite materials have generated plenty of interest due to the ability of a small quantity of filler material to significantly enhance the properties of the host polymer. We have demonstrated here the use of multi-walled carbon nanotubes oxidized by different methods as filler materials in the polymer matrix of poly[oligo(ethylene glycol)oxalate]. Both the host and filler material have been characterized thoroughly in terms of their thermal and structural properties. The nanotubes do not appear to have a significant impact on the thermal stability of the polymer. While some improvements were observed for certain filler loadings, no dramatic increases in thermal stability were observed. However, through analyses conducted using DSC, it was noted that the glass transition temperatures of these nanocomposite materials did not change significantly, contrary to expectations. In some cases, decreases in T_g were observed. This counterintuitive effect of the filler material on the polymer is attributed to several competing effects, with decreased crystallinity and residual solvent favouring a lowered T_g, while increased solid character and reduced flexibility of the polymer chains favour an increase. These competing effects result in insignificant changes in the conductivity of the polymer, suggesting that oxidized MWNTs may represent an ideal filler material to be used in polymer electrolytes.

Very little research has been performed using the polymer POEGO despite conductivities superior to many ionically conductive polymers. Using this methodology, several exfoliated nanocomposites could be prepared using different molecular weights of POEGO as well as with other highly conductive polymers such as poly[bis(methoxyethoxyethoxy)phosphazene] (MEEP), poly(oxymethylene-oxyethylene) (POMOE) and several polysiloxanes. Depending on the synthetic procedure for the desired polymer, the effectiveness of the *in situ* preparation of these exfoliated nanocomposites would vary. For the *in situ* preparation of the nanocomposites explored here, the solutions were heated in the refluxing process. This is an aspect of the synthesis for samples prepared by Method A that was not explored here. This heating could lead to improved solubility of the nanotubes and potentially improve the dispersion of the nanotubes in the polymer matrix.

The conductivity testing demonstrated a few important features of these polymer nanocomposites. It was noted that the method of preparation had a significant effect on the conductive properties of the materials. This suggests that heating could lead to improved dispersion as evidenced by the ionic conductivity of the samples prepared by the *in situ* preparation method. Furthermore, the level of oxidation is of particular interest. The

samples prepared with 20 wt% of the Hummers' oxidized nanotubes (Method 1B) were ionically conducting whereas samples prepared with only 10 wt% of the acid oxidized nanotubes (Method 1A) were mixed conductors. This suggests that either using the Hummers' oxidation method or prolonging the reaction time for acid oxidation would lead to the best candidates for solid polymer electrolytes. Based on the data presented, the ideal materials for use as solid polymer electrolytes would be samples containing between 5-10 wt% nanotubes prepared by Method1B or samples prepared with 10-20 wt% nanotubes prepared by Method 2A. Each of these samples was ionically conducting and demonstrated a visible improvement in mechanical stability, although quantitative measurements of mechanical properties remain a topic for future work.

6. Acknowledgement

We would like to thank the Natural Sciences and Engineering Research Council of Canada (NSERC), Canada Foundation for Innovation (CFI), Atlantic Innovation Fund (AIF) and University of Prince Edward Island (UPEI) for funding.

7. References

Ahir, S.V. (2007). Polymers containing carbon nanotubes: active composite materials, In: *Polymeric Nanostructures and their Applications;* Nalwa, H.S. (Ed.), pp. 153-200, American Scientific Publishers, ISBN 978-158830692, California.

Allcock, H.R.; Austin, P.E.; Neenan, T.X.; Sisko, J.T.; Blonsky, P.M.; Shriver, D.F. (1986) Poly phosphazenes with etheric side groups: prospective biomedical and solid electrolyte polymers. *Macromolecules*, Vol. 19, No. 6, pp. 1508-1512, ISSN 0024-9297.

Bouridah, A.; Dalard, F.; Deroo, D.; Cheradame, H.; LeNest, J.F. (1985) Poly(dimethyl-siloxane)-PEO based networks used as electrolytes in lithium electrochemical solid state batteries. *Solid State Ionics*, Vol. 15, No. 3, pp. 233-240, ISSN 0167-2738.

Chan, C.K.; Peng, H.; Liu, G.; McIlwrath, K.; Zhang, X.F.; Huggins, R.A.; Cui, Y. (2008a). High performance lithium battery anodes using silicon nanowires. *Nature*, Vol. 3, No. 1, pp. 31-35, ISSN 1748-3387.

Chan, C.K.; Zhang, X.F.; Cui, Y. (2008b). High capacity Li ion battery anodes using Ge nanowires. *Nano Lett.*, Vol. 8, No. 1, pp. 307-309, ISSN 1530-6984.

Croce, F.; Appetecchi, G.B.; Persi, L.; Scrosati, B. (1998) Nanocomposite polymer electrolytes for lithium batteries. *Nature*, Vol. 394, No. 6692, pp. 456-458, ISSN 0028-0836.

Dalton, A.B.; Collins, S.; Munoz, E.; Razal, J.M.; Ebron, V.H.; Ferraris, J.P.; Coleman, J.N.; Kim, B.G.; Baughman, R.H. (2003). Super-tough carbon-nanotube fibers. *Nature*, Vol. 423, No. 6941, ISSN 0028-0836.

Fergus, J.W. (2010). Ceramic and polymeric solid electrolytes for lithium-ion batteries. *J. Power Sources,* Vol. 195, No. 15, pp. 4554-4569, ISSN 0378-7753.

Gao, J.; Itkis, M. E.; Yu, A.; Bekyarova, E.; Zhao, B.; Haddon, R.C. (2005). Continuous spinning of a single-walled carbon nanotube-nylon composite fibre. *J. Am. Chem. Soc.*, Vol. 127, No. 11, pp. 3847-3854, ISSN 0002-7863.

Hall. R. (1967) Minimizing errors of four point probe measurements on circular wafers. *Journal of Scientific Instruments*, Vol. 44, No. 1, ISSN 0950-7671.

Hummers Jr., W.S.; Offeman, R.E. (1958). Preparation of graphitic oxide. *J. Am. Chem. Soc.*, Vol. 80, No. 6, pp. 1339, ISSN 0002-7863.

Iijima, S. (1991) Helical microtubules of graphitic carbon. *Nature,* Vol. 354, No. 6348, pp. 56-58, ISSN 0028-0836.

Iijima, S. (2001). Carbon nanotubes: past, present, and future. *Physica B*, Vol 323, No. 1, pp. 1-5, ISSN 0921-4526.

Khare, R.; Bose, S. (2005). Carbon nanotubes based composites - a review. *Journal of Minerals & Materials Characterization & Engineering,* Vol. 4, No. 1, pp. 31-46, ISSN 1559-2511.

Kojima, Y.; Usuki, A.; Kawasumi, M.; Okada, A.; Fukushima, Y.; Kurauchi, T.; Kamigaito, O. (1993). Mechanical properties of nylon 6-clay hybrid. *Mat. Res.*, Vol. 8, No. 5, pp. 1185-1189, ISSN 0884-2914.

Liu, P.; Gong, K.; Xiao, P.; Xiao, M. (2000). Preparation and characterization of poly(vinyl acetate)-intercalated graphite oxide nanocomposites. *J. Mater. Chem.*, Vol. 10, No. 4, pp. 933-935, ISSN 0959-9428.

Ma, P.-C.; Siddiqui, N.A.; Marom, G.; Kim, J.-K. (2010) Dispersion and functionalization of carbon nanotubes for polymer-based nanocomposites: a review. *Composites: Part A.*, Vol. 41A, No. 10, pp. 1345-1367, ISSN 1359-835X.

Meyer, W. (1998). Polymer electrolytes for lithium-ion batteries. *Adv. Mater.*, Vol. 10, No. 6, pp. 439-448, ISSN 0935-9648.

Mizushima, K.; Jones, P.C.; Wiseman, P.J.; Goodenough, J.B. (1980). Lithium cobalt oxide: a new cathode material for batteries of high energy density. *Mat. Res. Bull.*, Vol. 15, No. 6, pp. 783-789, ISSN 0025-5408.

Moniruzzaman, M.; Winey, K.I. (2006) Polymer nanocomposites containing carbon nanotubes. *Macromolecules*, Vol. 39, No. 16, pp. 5194-5205, ISSN 0024-9297.

Nazri, G.-A.; Pistoia, G. (Eds.). (2004) *Lithium Batteries: Science and Technology*, Kluwer Academic Publishers, ISBN 978-0387926742, Boston.

Paul, D.R.; Robeson, L.M. (2008). Polymer nanotechnology: Nanocomposites. *Polymer*, Vol. 49, No. 15, pp. 3187-3204, ISSN 0032-3861.

Rinzler, A.G.; Liu, J.; Dai, H.; Nikolaev, P.; Huffman, C.B.; Rodríguez-Macías, F.J.; Boul, P.J.; Lu, A.H.; Heymann, D.; Colbert, D.T.; Lee, R.S.; Fischer, J.E.; Rao, A.M.; Eklund, P.C.; Smalley, R.E. (1998). Large-scale purification of single-wall carbon nanotubes. Process, product, and characterization. *Appl. Phys. A,* Vol. 67, No. 1, pp. 29-37, ISSN 0947-8396.

Thackeray, M.M.; Davide, W.I.F.; Bruce, P.G.; Goodenough, J.B. (1983). Lithium insertion into manganese spinels. *Mat. Res. Bull.*, Vol. 18, No. 4, pp. 461-472, ISSN 0025-5408.

Tonge, J.S.; Shriver, D.F. (1989). Increased dimensional stability in ionic conducting polyphosphazenes systems. *J. Electrochem. Soc.*, Vol. 134, No. 1, pp. 269-270, ISSN 0013-4651.

Whittingham, M.S. (1976). Electrical energy storage and intercalation chemistry. *Science*, Vol. 192, No. 4244, pp. 1126-1127, ISSN 0036-8075.

Xu, W.; Belieres, J.-P.; Angell, C.A. (2001). Ionic conductivity and electrochemical stability of poly[oligo(ethylene glycol)oxalate]-lithium salt complexes. *Chem. Mater.*, Vol. 13., No. 2, pp. 575-580, ISSN 0897-4756.

Zeleznak, K.J.; Hoseney, R.C. (1987). The glass transition in starch. *Cereal Chemistry*, Vol. 64, No. 2, pp. 121-124, ISSN 0009-0352.

Zhang, R.; Hu, Y.; Li. B.; Chen. Z.; Fan. W. (2007). Studies on the preparation and structure of polyacrylamide/α-zirconium phosphate nanocomposites. *J. Mater. Sci.*, Vol. 42, No. 14, pp. 5641-5646, ISSN 0022-2461.

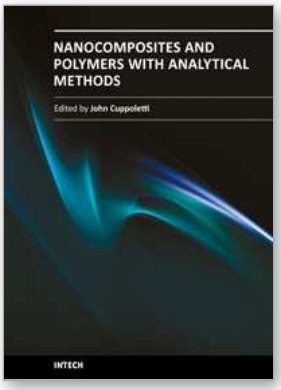

Nanocomposites and Polymers with Analytical Methods
Edited by Dr. John Cuppoletti

ISBN 978-953-307-352-1
Hard cover, 404 pages
Publisher InTech
Published online 09, August, 2011
Published in print edition August, 2011

This book contains 16 chapters. In the first part, there are 8 chapters describing new materials and analytic methods. These materials include chapters on gold nanoparticles and Sol-Gel metal oxides, nanocomposites with carbon nanotubes, methods of evaluation by depth sensing, and other methods. The second part contains 3 chapters featuring new materials with unique properties including optical non-linearities, new materials based on pulp fibers, and the properties of nano-filled polymers. The last part contains 5 chapters with applications of new materials for medical devices, anodes for lithium batteries, electroceramics, phase change materials and matrix active nanoparticles.

INTECH
open science | open minds

InTech Europe
University Campus STeP Ri
Slavka Krautzeka 83/A
51000 Rijeka, Croatia
Phone: +385 (51) 770 447
Fax: +385 (51) 686 166
www.intechopen.com

InTech China
Unit 405, Office Block, Hotel Equatorial Shanghai
No.65, Yan An Road (West), Shanghai, 200040, China
中国上海市延安西路65号上海国际贵都大饭店办公楼405单元
Phone: +86-21-62489820
Fax: +86-21-62489821